2013 IEEE/RSJ International Conference on
Intelligent Robots and Systems (IROS)
November 3-7, 2013. Tokyo, Japan

Automated Microfluidic System for Orientation Control of Mouse Embryos

Yong Kyun Shin[1], Yeongjin Kim[2] and Jung Kim[2]

Abstract— **Microinjection and biopsy of oocytes and embryos in Assisted Reproductive Technology (ART) require highly delicate handling of cells. In particular, efficient control of cell orientation is necessary to maintain their integrity during tool penetration, which currently remains challenging to accomplish by the existing method of repeated aspiration/release via micropipette. We present a microfluidic platform to automate the process of cell orientation control and trapping by means of hydrodyanmic force and vision-based position control. The device is accessible by conventional micropipettes via a cavity, allowing immobilized cells to be operated on. An orientation control algorithm based on the movement of the embryo within the microchannel is proposed. Visual tracking of the polar body is used to provide the information of cell orientation. Experimental results with mouse embryos indicate that cell orientation can be systematically controlled autonomously without human intervention and therefore provides a framework for further development of robotics approach to precise manipulation of microparticles within microfluidic devices.**

I. INTRODUCTION

Single cell manipulation techniques in Assisted Reproductive Technology (ART) have been developed for several decades and emerged as an important tool in clinical and biological research applications. According to Centers for Disease Control (CDC), 10% of all women in the United States suffer from infertility-related problems [1]. The treatments for these patients often involve ICSI, or intracytoplamic sperm injection, to carefully place a single sperm into an oocyte as part of *in vitro* fertilization (IVF) process [2]. In many cases, the procedure is followed by preimplantation genetic diagnosis (PGD) to selectively extract a polar body for genetic profiling and disease screening. In biological research, transgenic animals are created by microinjection of genetic materials for drug screening and study of human diseases [3]. A family of other ART applications such as embryo transfer (ET), nuclear transfer (NT) and gamete intrafallopian transfer (GIFT) also involve similar processes of targeted insertion of foreign species or removal from a specific cellular structure.

Due to the highly delicate nature of the embryos and the invasiveness of these cellular surgery operations, the orientation of vital cellular structures relative to the tool penetration path is critical to maintain their integrity. As shown in Fig. 1, the polar body is one such organ that contains an embryo's genetic information, whose orientation is directly related to its survial rate [4], [5]. During microinjection, for example, the polar body must be oriented in the image plane (in-plane, as shown in Fig. 1(a)) and away from the pipette. Unfortunately, conventional micromanipulation techniques rely on the manual control of micropipettes for reorientation by repeated aspiration/release of the embryo until the desired orientation is achieved. Due to the inherently limited manipulability offered by micropipettes, this process is inevitably stochastic, imprecise, labor-intensive and slow ($\geq$ 40 s per cell). These limitations represent the need for development of novel micromanipulation tools and systems for increased productivity.

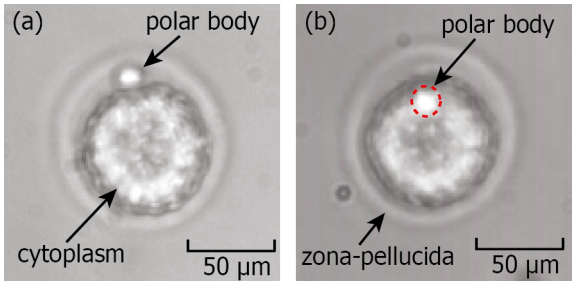

Fig. 1. Image of mouse embryo structures. (a) The round polar body is located in the image plane (in-plane) with respect to the cytoplasm and its orientation can be clearly identified. (b) the polar body is located out-of-plane with respect to the cytoplasm and the image plane and its location is difficult to identify.

Several robotics approaches capable of manipulating cell orientation have previously been proposed. On-chip robotics using non-contact, fully enclosed and magnetically actuated microtools is being developed by Hagiwara et al. [6], [7]. Although the thin manipulator arms could be used to perform various tasks including rotating against their tips, their movement was limited to planar motion, making accurate reorientation a difficult process. An array-based suction platform has been proposed in combination with a motorized stage for automated cellular injection by Liu et al.[8]. However, the degree-of-freedom in orientation control was also limited to a single axis. An automated approach for polar body reorientation by fluid propulsion in the holding micropipette has also been proposed [9]. In this work, the performance for cell immobilization was not addressed and this method could make successive cell searching difficult.

This paper presents an automated microfluidic system that is able to control the polar body orientation of mouse embryos by employing hydrodynamic forces. The benefit of using a cell conveying microfluidic device is the ability to control small volumes of liquid, allowing precise transport of

[1]Park Systems Corp., KANC 4F, Iui-Dong, 906-10, Suwon 443-270, Republic of Korea [2]Department of Mechanical & Aerospace Engineering, Korea Advanced Institute of Science and Technology (KAIST), Daejon, 305-701, Republic of Korea jungkim at kaist.ac.kr

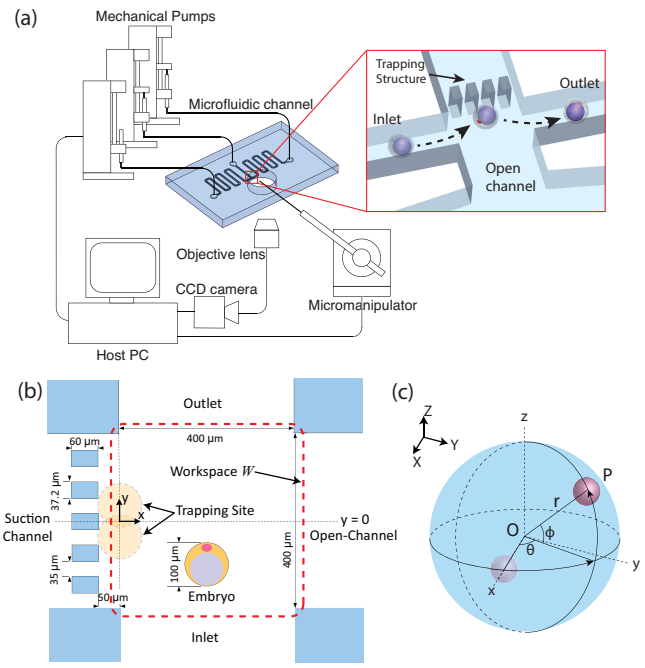

Fig. 2. Schematic illustration of (a) proposed microchannel, (b) system configuration and (c) coordinate description of the polar body orientation. The position of the polar body and the cell is denoted by points **P** and **O**, respectively.

individual cells sequentially and reducing the effort needed in sorting and searching for subsequent cells [10], [11]. The microchannel is designed to accommodate access of standard micropipettes and features transport channels (i.e. inlet and outlet) as well as suction channel for immobilization, intersecting in an orthogonal shape to form the manipulation workspace for reorientation. By analysing the rolling behaviour of round embryos within the channel, we implement a simple logic that "steers" the cell to the immobilization site in such a way to capture them in a specified orientation. Visual tracking of the polar body is used to provide orientation information for the control logic. This approach offers a generalized method for achieving systematic rotational motion within a microfluidic device while being compatible with simple cell conveying microchannels with tool access capability.

II. Methods

A. Microchannel Design

The proposed device is a single-layer PDMS microchannel that consists of an inlet, outlet, immobilization, and open-cavity channel as illustrated in Fig. 2(a). The open-cavity is produced by a round mechanical punch prior to plasma bonding of PDMS onto the glass substrate and serves as the access point for microtools. The fluid flow within each channel other than the open-channel is driven by a separate mechanical pump. The geometry at the channel intersection compared to mouse embryo is shown in Fig.2(b). The height of the channel is 200 μm. The thin rectangular cage-shaped structures in the suction channel are designed to trap cells

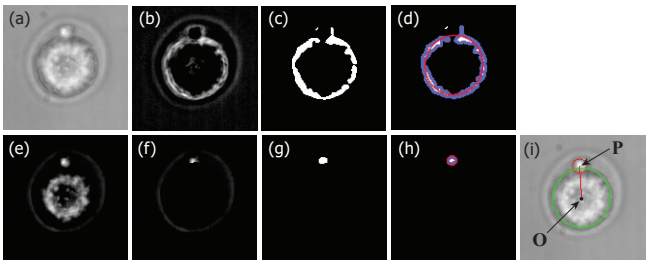

Fig. 3. Visual detection of the polar body and the cytoplasm. The algorithm detects the points **P** and **O** when the polar body is located in-plane, and only detects **O** when the polar body is located out-of-plane.

against and prevent them from entering the suction channel. The open-channel length is designed to accommodate the access of microtools, which normally have a horizontal tip length of approximately 500 μm. The orientation of the polar body of an embryo is described by the in-plane angle θ and out-of-plane angle ϕ as shown in Fig. 2(c).

B. Polar Body Orientation Estimation

Controlling the orientation of the polar body requires knowledge of of its current orientation described by θ and ϕ. For the in-plane orientation shown in Fig. 1(a), the polar body is clearly visible and its orientation may be determined to a moderate accuracy from finding θ alone by assuming negligible value of ϕ (the polar body is located in-plane). However, if the polar body is located out-of-plane ($\phi \neq 0$), its orientation cannot be determined from 2D microscopic image alone since ϕ cannot be determined. The problem is further complicated by the lack of image contrast between the polar body and the cytoplasm when they partially or fully overlap, as shown in Fig. 1(b). In order to continuously provide the information of cell orientation, we implemented a hybrid tracking strategy that consists of in-plane and out-of-plane tracking methods.

The image processing sequences for the in-plane polar body detection is shown in Fig. 3. The general approach described here is similar to [9]. First, background subtraction is used to obtain darker perimeter portion of the cytoplasm (Fig. 3(b)). The image is binarized (Fig. 3(c)). Contour tracking is then used to obtain the shape of the cytoplasm, at which point an ellipse is fitted in the least-squares sense [12] to obtain the cytoplasm shape and position (Fig. 3(d)). The identified cytoplasm is subsequently used as a mask to eliminate brighter regions of the cytoplasm from the lighter pixels in the image generated via background subtraction (Fig. 3(e),(f)). The remaining blob corresponds to the lighter center area of the polar body, which is identified via thresholding and contour finding (Fig. 3(g),(h)). The center of the cell (**O**) and the position of the polar body (**P**) are used to determine the in-plane angle (θ) and ϕ is assumed to be 0.

For the out-of-plane configuration, where the polar body blob is not detected or is too small, an approximate knowledge of cell's movement behavior within the microchannel is used to estimate the position of the polar body. Due to the higher density of the cell than the surrounding medium,

embryo sediments on the bottom of the microchannel and rotates as it travels, similar to a rolling ball. Using this observation, for a cell with radius r travelling in a straight path at an angle α for a distance d, the change in the orientation of the polar body between frames i and $i+1$ is estimated by the following coordinate transformation and a rotation matrix:

$$\mathbf{P}_O = \begin{vmatrix} P_x \\ P_y \\ P_z \end{vmatrix} = \begin{vmatrix} rcos(\phi)cos(\theta) \\ rcos(\phi)sin(\theta) \\ rsin(\phi) \end{vmatrix} \tag{1}$$

$$(\mathbf{P}_O)_{i+1} = \begin{vmatrix} c^2C+s^2 & cs(C-1) & -cS \\ cs(C-1) & c^2+s^2C & -sS \\ cS & sS & C \end{vmatrix} (\mathbf{P}_O)_i \tag{2}$$

where $c = cos(\alpha)$, $s = sin(\alpha)$, $S = sin((1-\lambda)d/r)$, $C = cos((1-\lambda)d/r)$.

Here, λ is a rate of slippage constant that we introduce to describe the rolling motion with the assumption that the slip-rate of the cell with respect to the glass substrate is constant and is defined as

$$\lambda = 1 - \frac{r\phi}{d}, \quad 0 \leq \lambda \leq 1 \tag{3}$$

C. Orientation Control Strategy

The proposed microchannel features an orthogonally shaped channel intersection that allows control of fluid in the x- and y-axes within the overlapping region. In order to manipulate the position of the cell to change its orientation prior to trapping, we implemented proportional feedback control of fluid velocity in each axis using the cell position $\mathbf{O}$ detected via image processing. The velocities in the inlet and outlet are equal in magnitude and opposite in direction. The spherical cell can thus be rolled to a desired location within the channel junction, where the objective is to accomplish a systematic and automated way of reaching the trapping site with the embryo having the desired orientation suitable for injection/biopsy. The problem formulated in this manner bears close resemblance to the classical ball-plate problem [13], where numerous path planning approaches have been proposed for applications such as spherical mobile robots and are available in the literature [14], [15], [16].

While these methods rely on the assumption that the spherical object of interest can be actuated without slipping or spinning about the vertical axis (i.e. pure rolling motion), our problem involves non-ideal case where cells are not fully round, the laminar velocity profile of microfluidic actuation generates some unwanted motion (i.e. spinning about z-axis near channel walls) due to non-uniform flow profile, and the space available for trajectory generation is finite. To circumvent these minor uncertainties and the limitation of out-of-plane orientation sensing, we devised an iterative algorithm that consists of a combination of two motion primitives: 1) translation with no orientation change, and 2) iterative in-plane rotation with no net change in the out-of-plane angle ϕ.

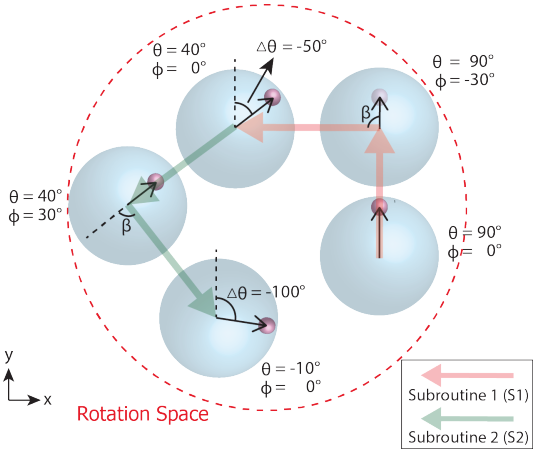

Fig. 4. Schematic illustration of the clockwise (CW) in-plane rotation method. The distance is not drawn to scale. The specified angular values are only for illustrative purposes and do not correspond to the actual values.

For pure translation, ϕ must be made to satisfy the condition $\phi = 0$ prior to the translation, and θ must be perpendicular to the direction of movement, as depicted on Fig. 4 (with $\theta = 90°$, $\phi = 0$). In this way, the rotation axis becomes aligned with the polar body and no change in the orientation would occur due to the movement. For the iterative in-plane rotation, the objective is to change θ without affecting ϕ in a limited workspace. To do this, two straight paths having a reflection pair (S1 and S2) are alternately executed as shown in Fig. 4. For S1, the length of the first roll in the direction of θ determines the magnitude of displacement of ϕ. Upon specified ϕ is reached, the second roll in the direction $\theta+\beta$ is executed until $\phi = 0$ is satisfied. The execution of two paths would result in the net displacement of θ only, whose magnitude is determined by the specified maximum ϕ and the angle β. The direction of in-plane rotation (clockwise or counter-clockwise) is determined by the sign of β. The S2 is similar to S1 except the direction of the first roll is $\theta + 180°$. Alternate execution of these subroutines are intended to reduce the space required for reconfiguration within the limited workspace.

Using the two motion primitives, an orientation control strategy is devised and its control logic is shown in Fig. 5. For practical reasons pertaining to microinjection, where the polar body orientation is often made to lie in the 12 o'clock position relative to a tool approaching from the 3 o'clock angle [4], the desired final orientation is chosen to be $(\theta, \phi) = (90°, 0°)$. For an arbitrarily located embryo, the algorithm first executes in-plane rotation to align θ with the horizontal axis (0° or 180°). In step 2, the polar body is vertically translated to the midplane ($y = 0$). This translation does not affect the cell orientation due to the in-plane rotation executed in step 1. Once the cell is located in the midplane with its polar body horizontally positioned, step 3 is executed to rotate the polar body to the final desired position, $\theta = 90°$. This rotation may slightly displace the cell in the vertical direction. Depending on the vertical location of the cell, step 4 translates the cell to the upper or lower trapping site near

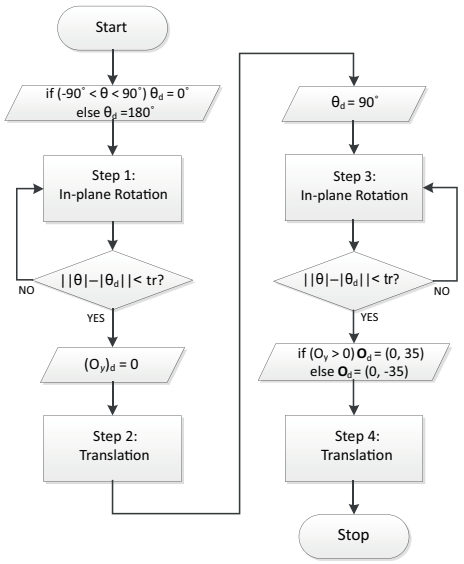

Fig. 5. Flow chart illustrating the control logic used for orientation control.

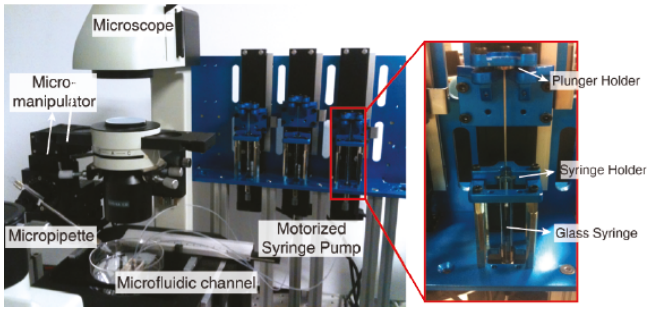

Fig. 6. Experimental setup of the proposed system. The image inset shows the glass syringe mounted on the syringe pump.

the midplane. Overall, the algorithm systematically changes the position or the orientation of the embryo sequentially to trap the cell in the desired configuration regardless of its initial location or orientation.

D. Experimental Setup

In order to drive the fluid flow within the microchannel, we used high-precision mechanical displacement pumps as shown in Fig. 6. The pump system consists of 3 linear guides (LX2005C, Misumi Corp., Japan) and step motors (RK545AA, Oriental Motor Corp., Japan) that have a minimum travel distance of 0.04 μm, corresponding to a dispensing volume of 67 pL using a 100 μL glass syringe. The small capacity precision glass syringes were used to minimize the perturbation and time-delay effects associated with mechanical compliance of a rubber plunger [17]. The pump system is controlled by a motion control board (PCI-7354, National Instruments Corp., USA) via a software developed in C++ using Visual Studio 2008 (Microsoft Corp., USA). An inverted microscope (AE31, Motic, China) with a CCD camera (SVS-Vistek, SVS340MUCP, Germany) having image size of 640×480 pixels is used with a frame rate of 60 Hz.

For preparing mouse embryo samples, six- to ten-weeks-old FVB female mice were superovulated by intraperitoneal injection of 5 IU of pregnant mare serum gonadotropin (PMSG, G4877, Sigma Corp., USA) to obtain a large number of eggs. Approximately 48 hours after the treatment, 5 IU of human chorionic gonadotropin (hCG, CG5, Sigma Corp., USA) was injected, and the mice were mated with fertile male mice overnight. Eggs were collected from the ampulla of the oviduct on the following morning and placed in M2 medium (M7167, Sigma Corp., USA). The cumulus corona cells were removed by treatment with hyaluronidase (H4272, Sigma Corp., USA) and washed thoroughly in M2 medium. Finally, the intact and fertilized oocytes (PN stage embryo) were stored separately in M2 medium.

III. Results and Discussions

A. Rotation Rate of Embryo

In order to determine the value of the slip constant λ, the rate of rotation of mouse embryo is measured in a straight channel having a width of 400 μm and a height of 200 μm. A mouse embryo with a diameter of approximately 100 μm is used. The measurement is performed by visually observing the location of the polar body within the cell. From the result shown in Fig. 7, it can be observed that the rate of rotation is dependent on the flow rate used. As the speed is increased, there is a tendency toward greater slip rate. This is likely caused by the imbalance between the translational drag force and the rotational torque imposed on the embryo by the laminar velocity flow profile [18], [19], although quantitative comparison of these forces within the narrowly bounded channel would require further investigation. For a flow rate of 3.0 μl/s, a full 1.5 revolution could not be recorded due to the high slip rate and the limited microscopic field-of-view. We note that the range of flow rates used by our system lies approximately within 3.0 μl/s. Since the out-of-plane polar body estimation does not involve more than approximately 50° rotation in a single direction in the orientation control algorithm and the distinction of the velocity-dependent rotation rate at this scale is rather minute, we chose the average value of λ to be 0.6.

B. Cell Position Control

Accurate and stable control of the cell position is important to implementation of the orientation control algorithm and to reduce error. For the purpose of evaluating the position control performance, a polymer microbead having 100 μm diameter (BB05N, Bangs Laboratories Inc., U.S.A.) suspended in M2 medium was used to represent the cell for ease of tracking by computer vision. Two circular reference trajectories with different radii are used as shown in Fig. 8. The speed of both trajectories were 150 μm/s. For the smaller circular path near the channel center, it can be observed that the cell position follows the round trajectory with good reproducibility, indicating stable motion and little deviation from the reference path in this region. The average tracking error for each frame is 26.66 μm. For the larger trajectory, the cell follows the path fairly well other than

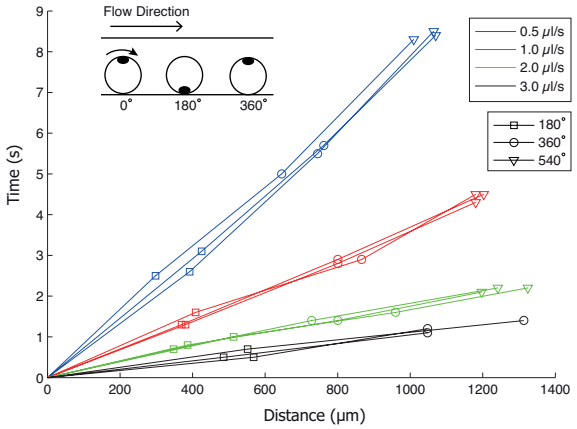

Fig. 7. Experimental measurement of cell rotation rate in a 1D channel with varying flow rates.

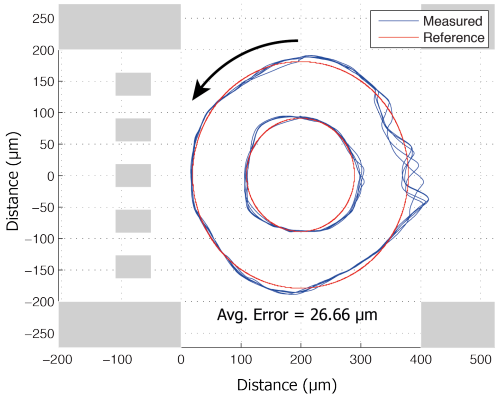

Fig. 8. Circular trajectory tracking performance evaluated using a polymer microbead.

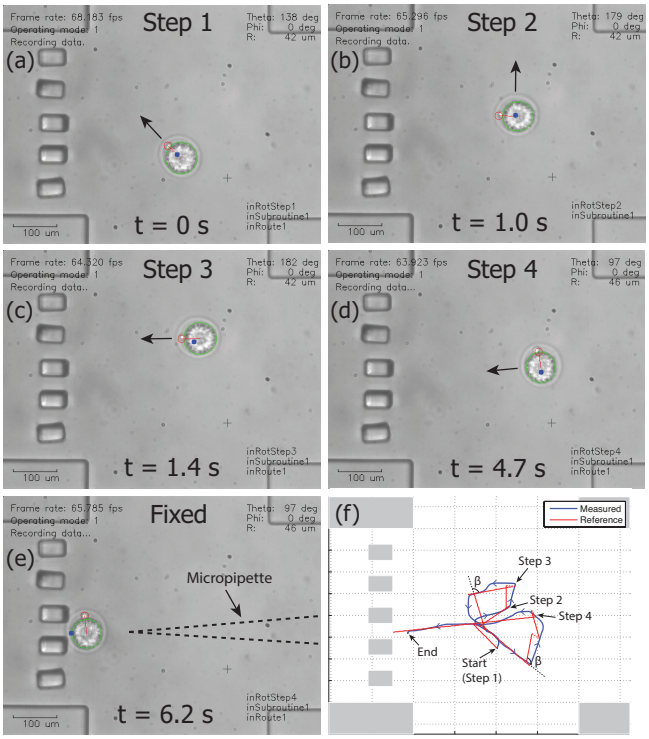

Fig. 9. Evaluation of the orientation control algorithm. (a) Embryo begins in-plane rotation to make $\theta = 180^\circ$ (b) Embryo translates to align vertical position prior to rotation. (c) Embryo begins in-plane rotation to make $\theta = 90^\circ$. (d) Once the final desired orientation is achieved, the embryo translates toward the trapping structure. (e) Embryo is fixed against the trapping structure and ready for manipulation. (f) Reference and measured embryo position history displaying the steps executed to reach the final desired position and orientation.

the open-channel region, where fluctuation and variation in the oscillatory behaviour are observed. This is due to the fact that the fluidic resistance in all other channels is fairly high and the flow rate through them are controlled by an independent pump. The small resistance helps to control fluid flow uniformly in the x-direction with a single pump connected to the suction channel (i.e. flow from suction channel exits entirely through the open-channel), but also slightly couples fluid movement between y- and x-axis near the entrance of the open-channel.

C. Orientation Control Performance

The performance of the proposed orientation control strategy was evaluated for the accuracy and the time required to reorient and trap cells, given an arbitrarily assigned initial location within the manipulation workspace. The initial value of θ was chosen randomly, while the value of ϕ was controlled to start from 0 (i.e. from in-plane) with point-and-click reference position adjustment to allow detection of the polar body at the onset of the trials. Fig. 9 shows time lapse images of a representative trial result. The values of β and maximum ϕ used were 110° and 35°, respectively. In step 1 , the polar body is aligned horizontally for translation in the vertical direction without orientation change. Step 2 then executes the vertical translation. Next, step 3 rotates the polar body to the desired final angle, $\theta_d = 90^\circ$. Translation to a nearby trapping structure in step 4 does not alter the angle for this configuration and the cell can be safely trapped for cellular surgery operation. Fig. 9(f) shows the reference signal and the trajectory taken by the embryo to move to the final trapping site. It can be observed that the space required to achieve reorientation is fairly small and remains bounded within W.

Table I shows the experimental results with varying initial conditions that successfully completed with the polar body near the desired position. The average time and angular error for the trial results was 11.5 s and 14°, respectively.

D. Discussions

The proposed orientation control algorithm made use of the iterative in-plane rotation step and pure translation step to devise a systematic method for reconfiguration of cell orientation. This simple approach was suited to our application since the motion of the cell within the microchannel, caused by complex fluid velocity profile dictated by the laminar flow and the channel geometry, do not entirely consist of rolling in the travelling direction. By decomposing each of the position and angular requirements into a series of steps and converging each variable in sequence, we minimized

TABLE I
ORIENTATION CONTROL RESULT.

	$[x_i(\mu\text{m}), y_i(\mu\text{m}), \theta_i(^\circ)]$	Time (s)	Error ($^\circ$)
T1	[165, 23, 224]	8.6	31
T2	[235, 55, 257]	17.6	11
T3	[175, -21, 303]	13.4	-8
T4	[104, 92, 154]	10.5	9
T5	[330, 124, 273]	12.5	21
T6	[329, -84, 201]	9.1	25
T7	[77, 12, 299]	13.3	6
T8	[160, 107, 45]	7.6	21
T9	[201, -75, 138]	6.2	7
T10	[200, 3, 250]	15.7	1

the accumulation of errors during the manipulation routine. Since the space required during the in-plane rotation was reduced by employing alternating S1 and S2 routines, the values of β and maximum ϕ could be chosen conservatively (i.e. $\beta \geq 110^\circ$, $\phi \leq 35^\circ$) to accurately align the angle θ to the desired value. Compared to the average time required for conventional pipetting method ($\geq$ 40 s), the proposed algorithm on average completed within a significantly shorter time of 11.5 s with adequate accuracy to discern the final polar body angle as the 12 o'clock position. A source of error for large angular variation cases resulted from the non-uniform alignment of immobilization structure during fabrication that resulted in the embryo coming to contact with one of the structure and rotating against it prior to trapping. For some cases, the residual angular displacement of ϕ from transition between step 3 and step 4 also translated to final error in θ.

IV. CONCLUSIONS

We presented a novel microfluidic system for autonomous orientation control of mouse embryos. By employing a microchannel featuring a relatively wide intersection area with cell trapping structures, we proposed the integrated concept of cell conveying microchannel with position control capability without additional components required, such as electrodes or pneumatic valves. From observation of the rolling behavior of the round cell within the microchannel, the position control concept was extended to a 3D orientation control problem by rolling the embryo in the vicinity of the trapping site. The proposed orientation detection and control algorithm demonstrated the ability to autonomously reconfigure and capture the mouse embryos within a significantly shorter time and adequate accuracy. Our robotics approach to noncontact manipulation of delicate embryos offers a generalized methodology on how reorientation of microparticles which demand precision and external tool-interaction may be implemented. Further development of the system would involve integration of initial orientation detection step to allow ϕ to start from arbitrary value (out-of-plane) and correctly understanding the forces acting on the spherical cell, thereby allowing a more effective and robust orientation control algorithm to be developed for increased efficiency.

ACKNOWLEDGMENT

This work was supported in part by Basic Science Research Program through the National Research Foundation of Korea (NRF) funded by the Ministry of Education, Science and Technology (2013-0026011).

REFERENCES

[1] "Center for disease control," http://www.cdc.gov/reproductivehealth/, accessed: 02/07/2012.
[2] A. Van Steirteghem, Z. Nagy, H. Joris, J. Liu, C. Staessen, J. Smitz, A. Wisanto, and P. Devroey, "High fertilization and implantation rates after intracytoplasmic sperm injection," *Human Reproduction*, vol. 8, no. 7, pp. 1061–1066, 1993.
[3] L. Ittner and J. Götz, "Pronuclear injection for the production of transgenic mice," *Nature protocols*, vol. 2, no. 5, pp. 1206–1215, 2007.
[4] G. Anifandis, K. Dafopoulos, C. Messini, N. Chalvatzas, and I. Messinis, "Effect of the position of the polar body during icsi on fertilization rate and embryo development," *Reproductive Sciences*, vol. 17, no. 9, pp. 849–853, 2010.
[5] L. Van der Westerlaken, F. Helmerhorst, J. Hermans, and N. Naaktgeboren, "Intracytoplasmic sperm injection: position of the polar body affects pregnancy rate," *Human Reproduction*, vol. 14, no. 10, pp. 2565–2569, 1999.
[6] M. Hagiwara, T. Kawahara, Y. Yamanishi, T. Masuda, L. Feng, and F. Arai, "On-chip magnetically actuated robot with ultrasonic vibration for single cell manipulations," *Lab on a Chip*, vol. 11, no. 12, pp. 2049–2054, 2011.
[7] M. Hagiwara, T. Kawahara, and F. Arai, "Local streamline generation by mechanical oscillation in a microfluidic chip for noncontact cell manipulations," *Applied Physics Letters*, vol. 101, no. 7, pp. 074 102–074 102, 2012.
[8] X. Liu, R. Fernandes, M. Gertsenstein, A. Perumalsamy, I. Lai, M. Chi, K. Moley, E. Greenblatt, I. Jurisica, R. Casper, *et al.*, "Automated microinjection of recombinant bcl-x into mouse zygotes enhances embryo development," *PloS one*, vol. 6, no. 7, p. e21687, 2011.
[9] C. Leung, Z. Lu, X. Zhang, and Y. Sun, "Three-dimensional rotation of mouse embryos," *Biomedical Engineering, IEEE Transactions on*, no. 99, pp. 1–1, 2012.
[10] A. Noori, P. Selvaganapathy, and J. Wilson, "Microinjection in a microfluidic format using flexible and compliant channels and electroosmotic dosage control," *Lab on a Chip*, vol. 9, no. 22, pp. 3202–3211, 2009.
[11] D. Delubac, C. Highley, M. Witzberger-Krajcovic, J. Ayoob, E. Furbee, J. Minden, and S. Zappe, "Microfluidic system with integrated microinjector for automated drosophila embryo injection," *Lab on a Chip*, 2012.
[12] A. Fitzgibbon, R. Fisher, *et al.*, "A buyer's guide to conic fitting," *DAI RESEARCH PAPER*, 1996.
[13] V. Jurdjevic, "The geometry of the plate-ball problem," *Archive for rational mechanics and analysis*, vol. 124, no. 4, pp. 305–328, 1993.
[14] R. Brockett and L. Dai, "Non-holonomic kinematics and the role of elliptic functions in constructive controllability," *Nonholonomic motion planning*, pp. 1–21, 1993.
[15] S. Bhattacharya and S. Agrawal, "Spherical rolling robot: A design and motion planning studies," *Robotics and Automation, IEEE Transactions on*, vol. 16, no. 6, pp. 835–839, 2000.
[16] M. Minor and J. Pukrushpan, "Motion planning for a spherical mobile robot: Revisiting the classical ball-plate problem," *Ann Arbor*, vol. 1001, p. 48109, 2002.
[17] J. Zhou, K. Ren, W. Dai, Y. Zhao, D. Ryan, and H. Wu, "Pumping-induced perturbation of flow in microfluidic channels and its implications for on-chip cell culture," *Lab Chip*, vol. 11, no. 13, pp. 2288–2294, 2011.
[18] H. Brenner, "The slow motion of a sphere through a viscous fluid towards a plane surface," *Chemical Engineering Science*, vol. 16, no. 3, pp. 242–251, 1961.
[19] M. Staben, A. Zinchenko, and R. Davis, "Motion of a particle between two parallel plane walls in low-reynolds-number poiseuille flow," *physics of fluids*, vol. 15, p. 1711, 2003.